THE UNIVERSITY of EDINBURGH

Edinburgh Research Explorer

Hybrid Dielectric Resonator Antenna for Diversity Applications with Linear or Circular Polarization

Citation for published version:
Kuznetcov, M, Podilchak, S, Clénet, M & Antar, YMM 2021, 'Hybrid Dielectric Resonator Antenna for Diversity Applications with Linear or Circular Polarization', *IEEE Transactions on Antennas and Propagation*, pp. 1 - 1. https://doi.org/10.1109/TAP.2021.3060034

Digital Object Identifier (DOI):
10.1109/TAP.2021.3060034

Link:
Link to publication record in Edinburgh Research Explorer

Document Version:
Peer reviewed version

Published In:
IEEE Transactions on Antennas and Propagation

General rights
Copyright for the publications made accessible via the Edinburgh Research Explorer is retained by the author(s) and / or other copyright owners and it is a condition of accessing these publications that users recognise and abide by the legal requirements associated with these rights.

Take down policy
The University of Edinburgh has made every reasonable effort to ensure that Edinburgh Research Explorer content complies with UK legislation. If you believe that the public display of this file breaches copyright please contact openaccess@ed.ac.uk providing details, and we will remove access to the work immediately and investigate your claim.

OPEN ACCESS

Download date: 23. Jul. 2021

This article has been accepted for publication in a future issue of this journal, but has not been fully edited. Content may change prior to final publication. Citation information: DOI 10.1109/TAP.2021.3060034, IEEE Transactions on Antennas and Propagation

Hybrid Dielectric Resonator Antenna for Diversity Applications with Linear or Circular Polarization

Maksim V. Kuznetcov, *Student Member, IEEE*, Symon K. Podilchak, *Member, IEEE*, Michel Clénet, *Senior Member, IEEE*, Yahia M.M. Antar, *Life Fellow, IEEE*

***Abstract*—This article presents a novel dielectric resonator antenna (DRA) with an 8-port feeding system offering gain and polarization diversity. The single-antenna unit is defined by a square arrangement of four aperture slots (ACSs), hybridized with the radiation of the dielectric resonator. Basically, an atypical feeding layout, realized by two microstrip transmission lines driving each of the four ACSs (thus requiring a total of 8 feed lines), allows for controlled excitation of the polarization. This resonator and feeder define the 8-port DRA, which, can offer linear polarization (LP), right-handed circular polarization (RHCP) or left-handed circular polarization (LHCP). Reflection coefficient and coupling values for different port excitation scenarios are also investigated for each polarization state of the L-band antenna. The maximum gain is about 5 dBic for LHCP or RCHP and 5 dBi when considering LP radiation. Such agility can be useful for the Global Navigation Satellite System (GNSS), for example, and other RF challenged environments where the dominant polarization is not known apriori. Other applications include duplex systems, wireless communications, and other phased arrays where gain or polarization diversity is of interest.**

***Index Terms*—Dielectric resonator antenna (DRA), polarization diversity, hybrid antenna, microstrip line, aperture coupled slots (ACSs).**

I. Introduction

DIELECTRIC resonator antennas (DRAs) have received considerable attention for different RF communication systems and satellite applications. They are generally compact, provide high radiation efficiencies, can be excited using various feeding techniques, and provide high gain. Recent developments focus on new types of DRAs including dual-band operation with high impedance bandwidth [1], new feeding techniques [2] and new shapes for the radiating elements such as the T-shape [3], L-shape [4], stair-shape [5], [6] and others. However, to achieve wide bandwidth with a compact design, the feeding system can be challenging. Moreover, difficulties can arise when trying to achieve wide bandwidth and high polarization diversity at the same time. This is because most DRA feeding systems are focused on the efficient excitation of only one type of polarization, being either linearly polarized (LP) or circularly polarized (CP).

Maxim Kuznetcov and S. K. Podilchak are with the Institute of Digital Communications, The University of Edinburgh, Edinburgh EH9 3JW, Scotland, United Kingdom. (e-mail: s.podilchak@ed.ac.uk).

Michel Clénet is with the Defense Research and Development Canada, DRDC, Ottawa ON K1N 1J8, Canada. (e-mail: michel.clenet@drdc-rddc.gc.ca).

Yahia M.M. Antar are with the The Royal Military College of Canada, Kingston ON K7K 7B4, Canada. (e-mail: antar-y@rmc.ca).

Manuscript received August 6, 2020; revised November 28, 2020. This work was supported by Defense Research and Development Canada (DRDC).

It is well known that the polarization of the generated far-field radiation pattern for a DRA is mostly dependent on its feeding mechanism. For example, one of the earliest and most common feeding systems to achieve CP over a wide beamwidth is the quadrature feed described in [7] where microstrip lines were positioned on the dielectric resonator to excite two orthogonal modes. In the same way the antenna described in [8] uses two vertical strips with quadrature phase excitation to excite TE_{111} and TE_{113} modes simultaneously to achieve CP. That DRA operated from about 2.7 GHz to 3.8 GHz where the reported maximum gain was 6.8 dBic and where the axial ratio was below 4 dB. The antenna also utilized a large (205 mm by 205 mm) ground plane to improve radiation performances. Similar feeding was employed in the DRA described in [6] where a bottom microstrip line fed a ground plane slot with a stair-like dielectric structure on the top aperture. The CP antenna achieved an axial ratio below 3 dB from 9.3 GHz to 10.3 GHz.

Other feeding approaches considered substrate integrated waveguide (SIW) technology [2], [9], [10] or even enforcing modes using different shaped resonators [4], [11], [12]. Such as in [11] an H-shaped resonator was presented with a side attached trapezoidal-like patch. In that structure, truncation and cuts allowed for better impedance matching and caused multiple resonances over frequency enabling antenna operation from 3.61 GHz to 6.85 GHz. Thus depending on the design approach, such mode excitations can be controlled enabling different dominant polarizations in the far-field.

Following this design flexibility, such polarization diverse DRAs are of interest and can offer a higher degree of freedom by ensuring two or more polarization states. These antennas can be used in wireless communication systems to minimize fading losses caused by multipath effects as well as satellite systems for geolocation. Diversity antennas can also offer frequency reuse when combined with polarization modulation techniques as reported in [13] - [15]. Using such polarization diversity, the antenna system can be less affected by different signals obstacles, improving the reliability and accuracy of the transmitting data.

For example, in [16], to reduce power consumption and the signal bit-error-rate (BER), a dynamic polarization diversity antenna system was implemented and compared. In that work [16], which mainly considered the signal-to-noise ratio (SNR), a method to switch between two antennas while only one antenna was activated was implemented. Another diversity scenario was reported in [17], where antennas with equal gain were used to distinguish between small scale and large scale fading signals. Due to the fluctuating signal strengths in [17],

0018-926X (c) 2021 Crown Copyright. Personal use is permitted. For any other purposes, permission must be obtained from the IEEE by emailing pubs-permissions@ieee.org.
Authorized licensed use limited to: University of Edinburgh. Downloaded on March 20,2021 at 09:44:49 UTC from IEEE Xplore. Restrictions apply.

This article has been accepted for publication in a future issue of this journal, but has not been fully edited. Content may change prior to final publication. Citation information: DOI 10.1109/TAP.2021.3060034, IEEE Transactions on Antennas and Propagation

the wake-up packet reception rate could be jeopardized, and by using antenna diversity, those effects can be mitigated.

An antenna switching approach could also be implemented using antennas with diverse gain [18]. In this methodology, if the signal level power drops for one polarization, signals received from another polarization state can be employed to recover the data link. Using this approach, one polarization state will be active at a certain time. Similarly an equal gain combiner (ECG) technique can be implemented [19], where the signals can be combined using all active polarization states.

Most of the recent findings in the literature report on single-antenna units for diversity applications with new multi-port feeding configurations whilst offering good isolation between the ports. Moreover, and by following the previously mentioned advancements in feeding approaches for DRAs, a few polarization diverse DRA structures have been reported with multiple port feeding or made reconfigurable with two or more polarizations. In particular, the structure described in [20], was a 2-port DRA using coplanar waveguide technology to excite two TE_{111} orthogonal modes. The antenna provided 7 % and 11.6 % bandwidth for port one and port two, respectively, with a maximum gain of 6.45 dBi for its two polarization states. Similarly, a two port dual-LP reconfigurable DRA was reported in [21]. The structure employed inverted-trapezoid patches and skywork switches along with applied phase shifts to the two ports to control the TE_{111} and TM_{111} modes for radiation from about 5 GHz to 6 GHz. This resulted in the control of the pattern while the reported maximum gain was 10.3 dBi at 5.5 GHz.

Advancing on these findings for antenna diversity and the aforementioned DRA feeding approaches, we report on a new 8-port antenna design achieving simultaneously dual-CP or dual-LP. The single-antenna unit is defined by a square arrangement of aperture coupled slots (ACSs) hybridized with the radiation of a cylindrical dielectric resonator to achieve polarization control. More specifically, two distinct microstrip lines drive each of the four ACSs (see Fig. 1), defining the 8-port antenna, for radiation of degenerate $HE_{11\partial}$ modes. To the best knowledge of the authors, no similar slot array feeding scheme, DRA concept and results have been reported. Basically it will be shown that high polarization diversity is possible for the proposed 8-port DRA allowing for the generation of various LP states, as well as RHCP and LHCP, by the appropriate excitation of the relevant ports.

It should be mentioned that some initial results were presented in [22]–[24]. In particular, simulated beam patterns and realized gain values were documented for some early prototypes to investigate antenna feasibility. In this paper, an expansion of these studies and new results are reported as well as complete measurements for the antenna structure in Fig. 1. It will be shown that the DRA provides high efficiency for its various polarization states (see Table I). Moreover, new and more efficient LP states are simulated and measured when compared to [22] by differential-like feeding. This paper also addresses inter-port coupling and antenna efficiency where it will be shown that values approaching 90 % are possible.

To demonstrate these concepts, two different, yet also similar, antenna structures are designed and examined for comparison having a center frequency of 1.5 GHz. Both offer an input impedance bandwidth of more than 40 % and distinct characteristics which may be of practical interest for diversity applications; for example, when requiring varied gain values for the different polarization states (Design A) as in [18], or, more consistent realized gain and matching over frequency when considering the possible LP and CP operational states (Design B). Both structures might be useful within the aforementioned systems [16]–[19], but depend on specific requirements of the antenna. However, results for Design B are fully reported herein, mainly due to its achieved antenna performances in terms of radiation efficiency, similar matching at the ports as well as its relatively consistent gains for the different polarization states. In the following regardless, both antennas are compared whilst measurements are provided, demonstrating proof-of-concept for the 8-port antenna concept.

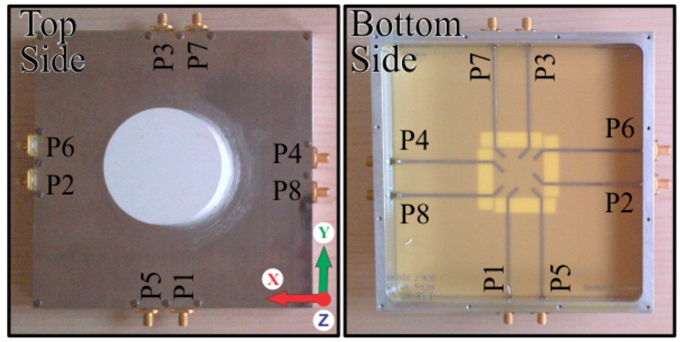

Fig. 1. Manufactured DRA: (left) The dielectric resonator element glued to the top metalized side which defines the ground plane platform. (right) The feeding network on the bottom side is shown with eight 50-Ω SMA connector jacks which excite the square array of four ACSs; i.e. two microstrip lines per slot defining the 8-port antenna.

TABLE I
FEED DEFINITIONS TO ACHIEVE THE POSSIBLE POLARIZATION STATES

Port	LP State 1 (Horizontal)	LP State 2 (Vertical)	RHCP	LHCP
P1	$1\angle 0°$	0	$1\angle 0°$	0
P2	0	$1\angle 0°$	$1\angle 90°$	0
P3	$1\angle 180°$	0	$1\angle 180°$	0
P4	0	$1\angle 180°$	$1\angle 270°$	0
P5	$1\angle 0°$	0	0	$1\angle 0°$
P6	0	$1\angle 0°$	0	$1\angle 270°$
P7	$1\angle 180°$	0	0	$1\angle 180°$
P8	0	$1\angle 180°$	0	$1\angle 90°$

II. ANTENNA DESIGN AND POLARIZATION CONSIDERATIONS

The proposed DRAs offer gain and polarization diversity which can be useful in communication or satellite systems such as the Global Navigation Satellite System (GNSS). Basically, in these scenarios, the proposed diversity antennas can support signal processing approaches [16]–[19] to improve overall system performance whilst employing only a single antenna unit.

The hybrid DRAs, Design A and Design B (see Figs. 1 and 2) consist mainly of three parts: (1) the dielectric resonator with ε_r = 10, radius and height of 31.75 mm and 22 mm,

0018-926X (c) 2021 Crown Copyright. Personal use is permitted. For any other purposes, permission must be obtained from the IEEE by emailing pubs-permissions@ieee.org.
Authorized licensed use limited to: University of Edinburgh. Downloaded on March 20,2021 at 09:44:49 UTC from IEEE Xplore. Restrictions apply.

This article has been accepted for publication in a future issue of this journal, but has not been fully edited. Content may change prior to final publication. Citation information: DOI 10.1109/TAP.2021.3060034, IEEE Transactions on Antennas and Propagation

respectively, glued on top of the four ACSs; (2) the FR-4 substrate with thickness h = 0.8 mm and ε_r = 4.3; and (3) eight 50-Ω microstrip lines which are perpendicular to the four ACSs and angled 45° at the open stub terminations. Details on the optimized dimensions for the two designs and the layout parameters can be seen in Fig. 2 and Table II.

In the next sections, the external feeding system and these two different antenna designs will be reported in detail: Design A and Design B. The former offers different peak antenna gains for its different polarization states while the latter offers similar antenna matching values at all its eight ports with consistent gain values. This is because the structure, Design B, is symmetric. Regardless, depending on the specific polarization or gain diversity application, Design A or Design B may be more suitable. As further described in Table I, each polarization state of the DRA is made possible by exciting different ports and applying the relevant phase shifts. In addition, both Design A and Design B were optimized using the commercial full-wave simulator Ansys HFSS and CST microwave Studio. HFSS was mainly used to refine the structure dimensions and simulate the radiation performances, while CST was used to compute the active S-parameter (or F-parameter) response, beam patterns, realized gain, and antenna efficiency.

A. External Feeding Approach to Achieve LP or CP

To generate circularly polarized radiation, approximately phased signals need to be applied to ports 1 to 4 or ports 5 to 8; i.e. an applied phase delay of 90° is required. Similarly, for the LP states, the DRA needs to be excited using ports 1, 3, 5, 7 or 2, 4, 6, 8 with a 0° and 180° phase shift; i.e. differential. To achieve these phase shifts different combinations of external hybrid couplers can be used, defining a supporting coupler system. The simplest implementation could be one 180° coupler and two 90° couplers for the CP states. For LP, only one hybrid coupler with a 180° output phase difference is required.

Possible circuit schematics are detailed in Fig. 3 for the CP and LP cases and examples of such couplers can be found in [25] or [26]. For simplicity, the coupler system from [27] (see specifically Fig. 5, from [27]) was employed for the DRA measurements in this paper; i.e. for the fabricated antenna prototype as in Fig. 1, enabling polarization diversity. Moreover, this external 5-port coupler system offered reduced imbalances at the ports from about 1 to 1.8 GHz. For example, the magnitude imbalance is less than about 1 dB over the majority of this frequency range whilst offering the required 90° sequential rotation [27].

B. Antenna Operation: Design A

1) Circular Polarization: RHCP (P1 to P4), LHCP (P5 to P8): During the simulations and structure optimizations in HFSS, the relevant dimensions near the ACSs for the 50-Ω microstrip lines were varied such that ports 1 to 4 provided the best possible matching (see Fig. 4(a)), while still making it possible to operate the antenna when using ports 5 to 8 for the other polarization state. As a result, the RHCP state provided better active F-parameter matching when compared to the LHCP state (see Figs. 4(b) and 5(a), respectively). For example, the active F-parameters for the RHCP state showed a -10 dB matching (or better) over a bandwidth from about 1 to 1.6 GHz, while LHCP was only able to reach -9 dB from 1.05 to 1.45 GHz with only -8 dB at the center frequency of 1.5 GHz. Since the coupling to the non-active ports is minimized at the 1.5 GHz design frequency, whilst good matching is achieved for the RHCP state, an efficiency maximum of 82 % can be achieved. On the other hand, an efficiency of 74 % is possible for the LHCP state (see Figs. 4(b) and 5(a)). Consequently, maximum realized gains for the RHCP state reached 4.9 dBic, while the LHCP state only reached 3.2 dBic (see Table III).

This general design goal for Design A, to achieve a higher CP gain for one polarization state, impacted the matching for ports 5 to 8; i.e. the reflection coefficient values (passive) were about -7 dB over the operating band of the DRA (see Fig. 4(a)). As expected, the active LHCP state is also not well matched; i.e. the active F-parameters are greater than -10 dB (see Fig. 5(a)). Looking at the simulated beam patterns for the LHCP and RHCP states (see Fig. 6) the diversity in the CP gains can be observed. Also, for both RHCP and LHCP, the cross-polarization level is well below -50 dBic at broadside.

2) Linear Polarization: Horizontal (P1, P3, P5, and P7) Vertical (P2, P4, P6, and P8): In this approach, only two ACS will are made active. This differential feeding, as outlined in Table I, offered the most efficient radiation for the LP states (and when also compared to the scenario when only one feed line per slot was driven for LP; i.e. port 1 or 5, and ports 2 or 6, as well as the other possible configurations for LP). For example, by following Table I, a radiation efficiency of 88 % at 1.5 GHz can be observed (see Fig. 5(b)). The simulations of the F-parameters also confirm that the active reflection coefficient reaches -20 dB at the design frequency for ports 1 and 3 or ports 2 and 4. Similar to the LHCP state, ports 5, 6, 7 and 8 were actively matched with values of about -7 dB. Also, simulated beam patterns in Fig. 6 show that the cross-polarization level is well below -15 dBi with the maximum realized gain at 1.5 GHz as expected.

Using this design approach, different gains for the different polarization states can be achieved defining a type of antenna offering polarization-gain diversity. As can be observed in the plot of the realized gain for the different polarization cases as in Fig. 7(a), a diversity gain of about 2 dB can be achieved for Design A at its center frequency of 1.5 GHz.

C. Antenna Operation: Design B

1) Circular Polarization: RHCP (P1 to P4), LHCP (P5 to P8): For Design B the microstrip terminations near the ACSs

TABLE II
DRA DIMENSIONS (ALL VALUES IN MILLIMETERS, SEE FIG. 2)

	W_g	H_F	H_S	H_R	D_R	W_S	L_S	SO_x	SO_y
Design A	160	0.762	0.035	22	63.5	8.8	36	19.4	4
Design B	160	0.762	0.035	22	63.5	8.8	36	19.4	4
	W_F	FO_{ya}	FO_{yb}	FO_x	FS	SA	L_{sa}	L_{sb}	
Design A	1.45	3.275	14.475	16.75	17.75	45°	7.5	8.3	
Design B	1.45	5.675	12.775	16.75	18.45	45°	7.5	8.5	

0018-926X (c) 2021 Crown Copyright. Personal use is permitted. For any other purposes, permission must be obtained from the IEEE by emailing pubs-permissions@ieee.org.
Authorized licensed use limited to: University of Edinburgh. Downloaded on March 20,2021 at 09:44:49 UTC from IEEE Xplore. Restrictions apply.

This article has been accepted for publication in a future issue of this journal, but has not been fully edited. Content may change prior to final publication. Citation information: DOI 10.1109/TAP.2021.3060034, IEEE Transactions on Antennas and Propagation

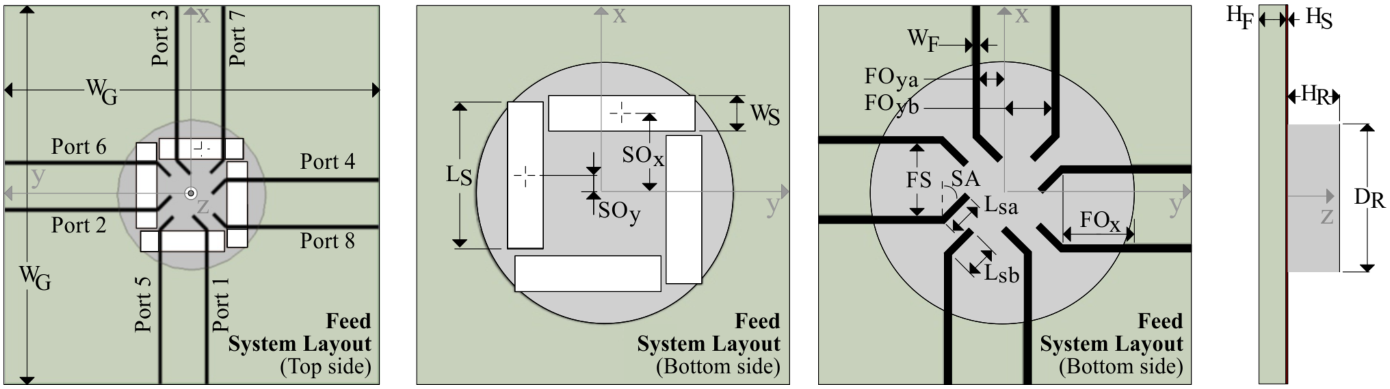

Fig. 2. Top, bottom and side layout views of the proposed DRAs (relevant to both Designs A and B). Dimensional details are described in Table II.

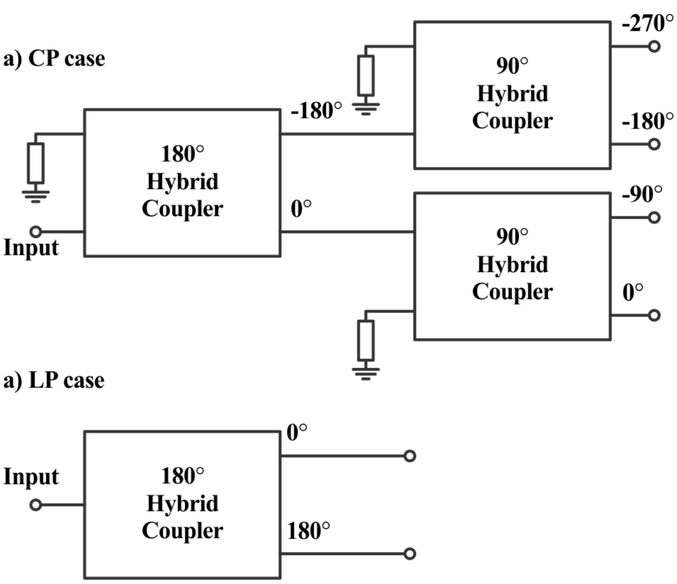

Fig. 3. Possible circuit combinations to generate CP, (a), where one 180° and two 90° hybrid couplers are required, and (b), LP, where only 180° coupler is needed. As further described in the text, a 5-port coupler system (see Fig. 5 from [27]) can be employed for both CP or LP DRA measurements. For example, for LP measurements, the 0° and 180° output circuit ports are only needed, from (a), while the -90° and -270° ports can be terminated in matched loads. Phased matched cables are also required when connecting this type of external coupler system to the appropriate ports of the DRA (see Table I).

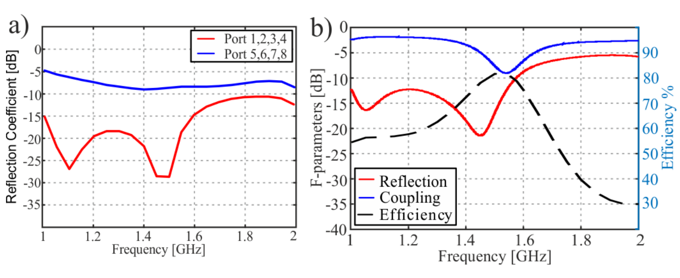

Fig. 4. Design A: (a) Simulated reflection coefficients (passive) for all eight ports. Reflection coefficient values for ports 1 to 4 are below -10 dB over entire range, however matching for ports 5 to 8 did not reach -10 dB. (b) The F-parameters and antenna efficiency for the RHCP state (ports 1 to 4).

slots were optimized to achieve similar passive matching at all the ports whilst achieving port coupling (passive) well below -15 dB for the ports connected to non-parallel microstrip feed

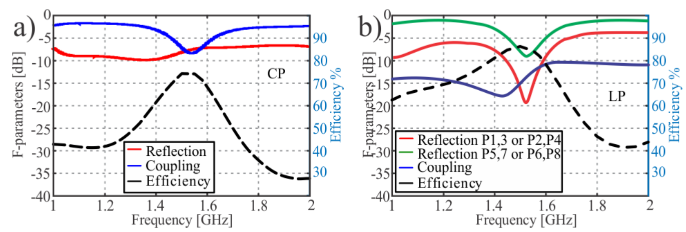

Fig. 5. Design A: (a) simulated active S-parameters (or F-parameters from CST defining the active reflection coefficient in dB as well as the coupling to the non-activated ports) for the LHCP state (ports 5 to 8). It can be observed that increased reflections are generated for the active S-parameters when compared to the RHCP state (see Fig. 4(b)). (b) Simulated F-parameters for the LP states (Horizontal: Ports 1, 3, 5, and 7; Vertical: Ports 2, 4, 6, and 8). The antenna is matched better for the horizontal state.

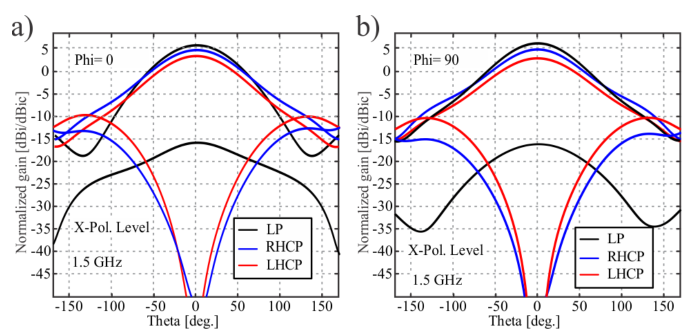

Fig. 6. Design A: simulated beam patterns and cross-polarization levels for the antenna operating states as defined in Table I in the (a) $\phi = 0°$ and (b) $\phi = 90°$ planes. As mentioned, Design A provides variation of the gains for its different polarization states.

lines (see Figs. 8 and 9).

As a result, the RHCP and LHCP states can also provide consistent active F-parameters (see Fig. 12(a)). Overall, the F-parameters showed a -10 dB (or better) impedance matching over a bandwidth from 1.1 to 1.55 GHz. Additionally, the coupling to the non-activated ports is minimized at the 1.5 GHz design frequency. This results in an efficiency maximum of 80 % (see Fig. 12(a)). This is related to the fact that two microstrip lines feed the same ACS, defining the proposed co-located antenna feeding structure. Also, by using this symmetric feeding approach the realized gain for the DRA is consistent for both CP states; i.e. simulated realized gain

0018-926X (c) 2021 Crown Copyright. Personal use is permitted. For any other purposes, permission must be obtained from the IEEE by emailing pubs-permissions@ieee.org.
Authorized licensed use limited to: University of Edinburgh. Downloaded on March 20,2021 at 09:44:49 UTC from IEEE Xplore. Restrictions apply.

This article has been accepted for publication in a future issue of this journal, but has not been fully edited. Content may change prior to final publication. Citation information: DOI 10.1109/TAP.2021.3060034, IEEE Transactions on Antennas and Propagation

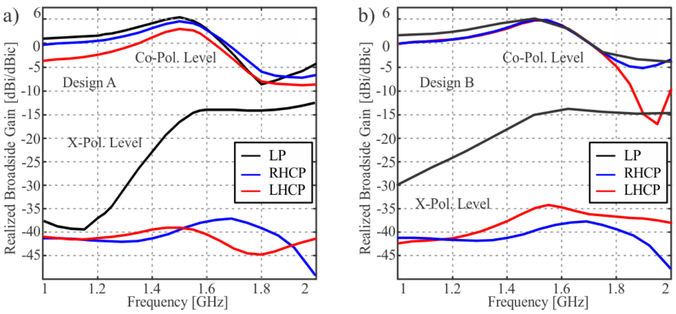

Fig. 7. Simulated realized gain versus frequency for Design A (a) and Design B (b) considering the defined port definitions in Table I. It should be mentioned that Design A (a) provides different realized gain for its states, while Design B (b) achieves consistent gain values of about 5 dBi and 5 dBic at 1.5 GHz.

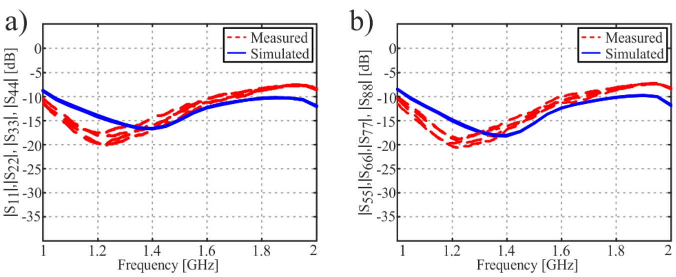

Fig. 8. Design B: simulated and measured reflection coefficients (passive) for all eight ports. Reflection coefficient values are -14 dB at the 1.5 GHz design frequency. It is important to note that the reflection coefficients for all eight ports are consistent. This is due to the symmetric antenna structure.

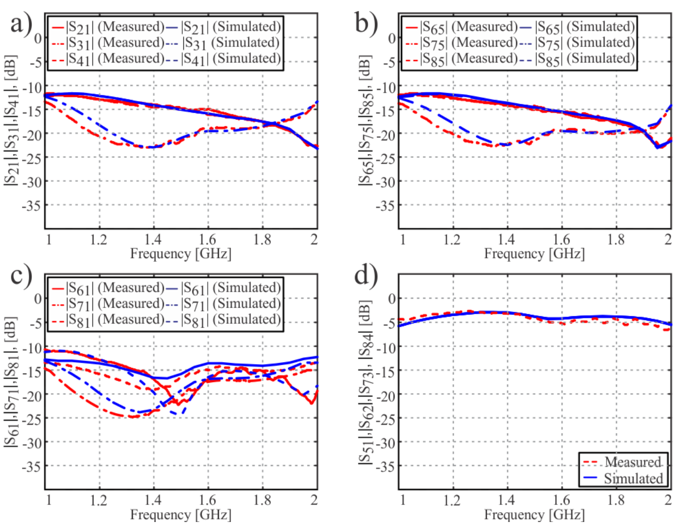

Fig. 9. Design B: simulated and measured passive coupling between the ports. Coupling values are about -15 dB or below at 1.5 GHz (a)-(c), except for cases when the ports are connected to microstrip lines which feed the same slot (d).

peaks were about 5 dBic for the LHCP and RHCP states, respectively, as reported in Fig. 7(b).

2) Linear Polarization: Horizontal (P1, P3, P5, and P7) Vertical (P2, P4, P6, and P8): The F-parameters for the LP states are presented in Fig. 12(b) and generally provide a more narrow -10 dB impedance bandwidth when compared to the CP states for Design B in that the structure is only well matched from 1.45 to 1.55 GHz. Additionally, the coupling is generally lower than the CP configurations over the operating band of the antenna while the maximum antenna efficiency is 88 % at 1.5 GHz.

The antenna simulations also suggest that high polarization purity is possible. This is because low cross-polarization levels of -20 dB or better can be observed for the LP states at broadside (see Fig. 13). Similarly for RHCP and LHCP. Also, the simulated beam patterns in Fig. 13 suggest that the half-power beam width (HPBW) is approximately 85° while the maximum realized gain is more than 5 dBi at 1.5 GHz (see Fig. 7(b) and Table IV).

TABLE III
DESIGN A: SIMULATION RESULTS FOR THE POLARIZATION STATES

Pol. State	Max Gain (Real.)	X-pol. Level ($\theta = 0°$)	3dB HPBW	Rad. Eff.	Active Impedance Matching at 1.5 GHz
RHCP	4.9 dBic	<-50 dB	85°	81 %	P5,6,7,8 -17 dB
LHCP	3.2 dBic	<-50 dB	83°	74 %	P1,2,3,4 -8 dB
LP (Hor.)	5.3 dBi	<-18 dB	81°	88 %	P1,3 -14.8 dB P5,7 -8 dB
LP (Ver.)	5.3 dBi	<-18 dB	81°	88 %	P2,4 -14.8 dB P6,8 -8 dB

TABLE IV
DESIGN B: SIMULATION RESULTS FOR THE POLARIZATION STATES

Polarization State	Max Gain (Real.)	X-pol. Level ($\theta = 0°$)	3dB HPBW	Rad. Eff.	Active Impedance Matching at 1.5 GHz
RHCP	4.9 dBic	<-50 dB	85°	80 %	P5,6,7,8 -12 dB
LHCP	4.8 dBic	<-50 dB	83°	80 %	P1,2,3,4 -12 dB
LP (Hor.)	5.2 dBi	<-20 dB	81°	88 %	P1,3,5,8 -14 dB
LP (Ver.)	5.2 dBi	<-20 dB	81°	88 %	P2,4,6,8 -14 dB

III. MEASUREMENTS AND DISCUSSIONS

To validate the proposed diversity antennas, Design A and Design B were both manufactured and measured. Figs. 10 and 11 illustrate the full measurement setup considering the employed 5-port external coupler system (see Fig. 5 from [27]), the placement of the required dividers, and the proposed DRA with its relevant port connections.

Results for Design B are fully reported in this section. This is because Design B offers better matching for both of its LP states. On the other hand, the RHCP state for Design A offers best matching as well as higher gain and efficiency when compared to its LHCP state making the proposed antenna (i.e. Design A) suitable for diversity gain scenarios [18]. This enables a co-located antenna system, and thus, does not require the need to switch between antennas with different realized gains. Conversely, Design B offers good matching for all its ports and consistent gains for its LP and CP states making it suitable for perhaps polarization diversity applications as in [16], [17] and [19] and where a single-antenna unit is required. This can enable lower system implementation costs.

The S-parameters (passive) for Design A and B were measured using an Anritsu 37377C Vector Network Analyzer and results are in agreement with the simulations (see results in Figs. 8 and 9). Far-field antenna measurements were completed in the anechoic chamber facilities at The Royal Military College of Canada and values show a good agreement with the full-wave simulations (see Figs. 12-17). Given this experimental setup, particular measured realized gain patterns were plotted for different azimuth angles as well as the antenna response with respect to frequency. Beam

0018-926X (c) 2021 Crown Copyright. Personal use is permitted. For any other purposes, permission must be obtained from the IEEE by emailing pubs-permissions@ieee.org.
Authorized licensed use limited to: University of Edinburgh. Downloaded on March 20,2021 at 09:44:49 UTC from IEEE Xplore. Restrictions apply.

This article has been accepted for publication in a future issue of this journal, but has not been fully edited. Content may change prior to final publication. Citation information: DOI 10.1109/TAP.2021.3060034, IEEE Transactions on Antennas and Propagation

patterns, the matching and the coupling responses, axial ratios, and cross-polarization levels are also reported.

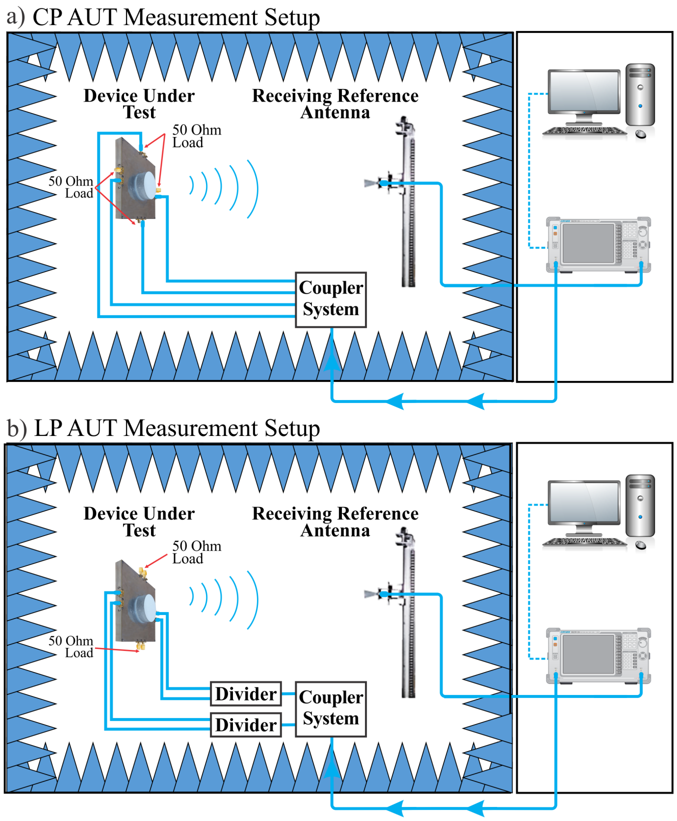

Fig. 10. Measurement setup for the CP, (a), and the LP cases, (b). Both show the required DRA and circuit connections with reference to the antenna ports (see also Fig. 11). Note: for the LP measurement cases, dividers are also required.

A. Port Matching, Coupling & Feeding Considerations

Measured and simulated passive S-parameters are presented in Figs. 8 and 9 for Design B. Results indicate that the DRA offers a good impedance bandwidth with reflection coefficients below -10 dB from 1.1 to 1.8 GHz (which is more than 40 %). The coupling between ports 3 and 1 is also below -15 dB over the entire frequency range while the coupling between ports 1 and 2 is below -10 dB (see Fig. 9(a)). This increase in coupling is related to the port locations; i.e they are opposite to each other. In a similar way ports 6, 7, and 8 have coupling values to port 1 below -10 dB. However, the inter-port coupling between the microstrip lines which drive the same ACS can reach up to -4 dB (see Fig. 9(d)). This is consistent with the simulations for both Design A and Design B (all results not reported for brevity).

It is also important, to follow the port definitions as described in Table I for the various polarization states. This is because after significant comparisons and simulation trials (not fully reported here for simplicity), these port definitions offered the best radiation efficiency performances for all the defined polarization states as well as improved matching, reduced coupling and when the active S-parameters or F-parameters were considered as in Fig. 4(b), 5, and 12 and in Tables III and IV for the same DRA structure.

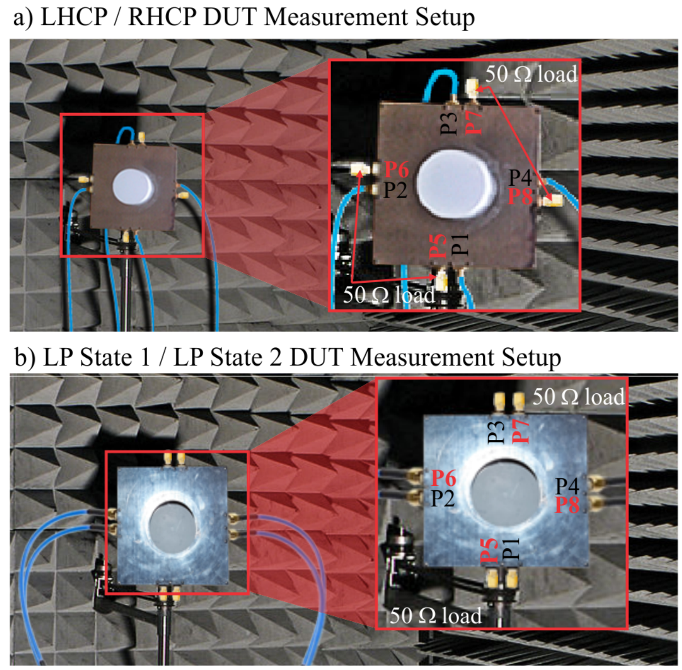

Fig. 11. DRA port connections considering the CP and LP states with external coupler feeding (see Fig. 10). For example, in (a), P1 to P4 are active, while P5 to P8 are loaded with 50-Ω defining the RHCP case, while in (b), P2, P4, P6, and P8 are active defining the vertical LP state (see Table I). Other polarization states are possible by selecting the appropriate output ports of the coupler system whilst connecting the DRA ports.

B. CP Antenna Operation: RHCP and LHCP

The antenna simulations and measurements demonstrate high polarization purity with low cross polarization levels at broadside for every CP state (see Figs. 13-16). For Design A and B, the different CP gain values can be observed in Fig. 14 for the RHCP and LHCP states, respectively. Also, the measured maximum realized gain is about 5 dBic at 1.5 GHz for Design B (both polarization states) and the antenna offers a HPBW of approximately 80° (see Figs. 14(b) and 15, respectively). Measured axial ratios are also well below 3 dB considering an angular range of more than ±50° as reported for different azimuth angles in Fig. 16. In general, the simulation results are in close agreement with the measurements.

C. LP Antenna Operation: Horizontal and Vertical

For Design B the antenna simulations and measurements demonstrated cross polarization levels of -15 dBi or less at broadside for every LP state (see Fig. 17). Measured maximum realized gain is at 1.5 GHz with a value of almost 5 dBi which is consistent with the simulations as reported in Table IV. Additionally, the realized gain over frequency is shown in Fig. 17(a) while the HPBW is approximately 88° as observed in Fig. 17(b).

D. General Discussions

Discrepancies between simulations and measurements for Design A and Design B could be related to manufacturing

0018-926X (c) 2021 Crown Copyright. Personal use is permitted. For any other purposes, permission must be obtained from the IEEE by emailing pubs-permissions@ieee.org.
Authorized licensed use limited to: University of Edinburgh. Downloaded on March 20,2021 at 09:44:49 UTC from IEEE Xplore. Restrictions apply.

This article has been accepted for publication in a future issue of this journal, but has not been fully edited. Content may change prior to final publication. Citation information: DOI 10.1109/TAP.2021.3060034, IEEE Transactions on Antennas and Propagation

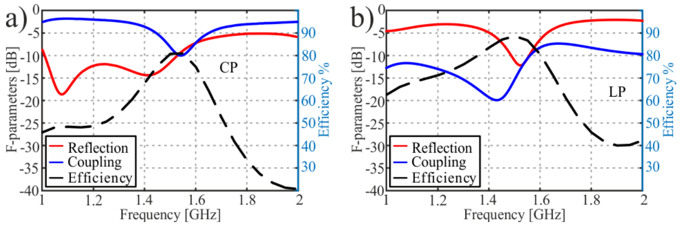

Fig. 12. Design B: simulated active S-parameters (or F-parameters from CST) defining the active reflection coefficient in dB as well as the coupling to the non-activated ports for the CP (a) and LP (b) states. The efficiency is also reported in (a) where it is observed that when the coupled power to the non-active ports is reduced, antenna efficiency increases. In addition, the active reflection coefficients demonstrate values of -10 dB (or less) at 1.5 GHz.

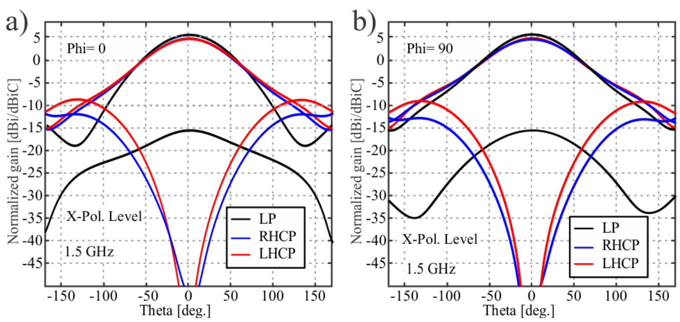

Fig. 13. Design B: simulated beam patterns and cross-polarization levels for the antenna operating states as defined in Table I.

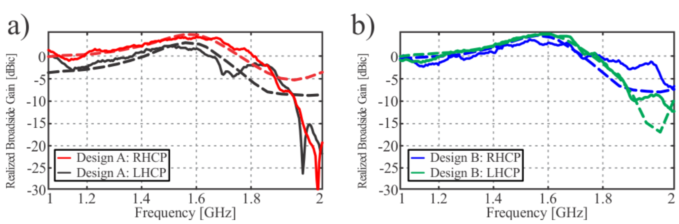

Fig. 14. Design A (a) and Design B (b) simulated and measured broadside gain versus frequency for the RHCP and LHCP states. Simulations and measurements are continuous and dashed lines, respectively.

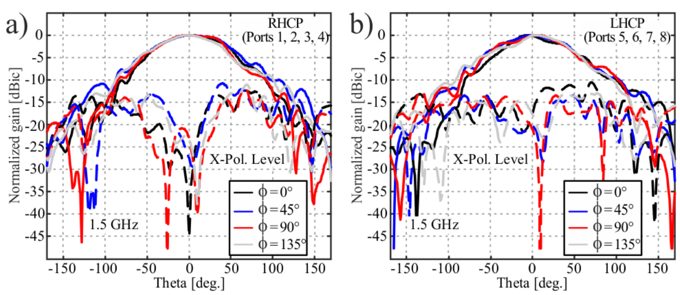

Fig. 15. Design B: RHCP (a) and LHCP (b) measured beam patterns at 1.5 GHz. Cross-polarization levels are also shown.

tolerances or by imbalances in the power combiners and external hybrid couplers employed to generate the required phase shifts at the ports (see Table I). More specifically, in the simulations the applied port voltages (magnitude and phase) were considered ideal.

It should also be mentioned that slightly higher than expected cross-polarization levels were observed in the measurements. For example, the simulated cross-polarization levels for the CP states are 50 dB below the main co-polarized maximum at broadside (see Fig. 13), while the measured cross-pol. range is about -15 dB to -45 dB (see Fig. 15). This is likely related to the employed CP reference antenna, in particular the cavity-backed spiral antenna from Steatite [28]. This commercial antenna has a relatively high cross-polarization value (about 10 dB below the main co-pol. beam maximum) at L-band frequencies.

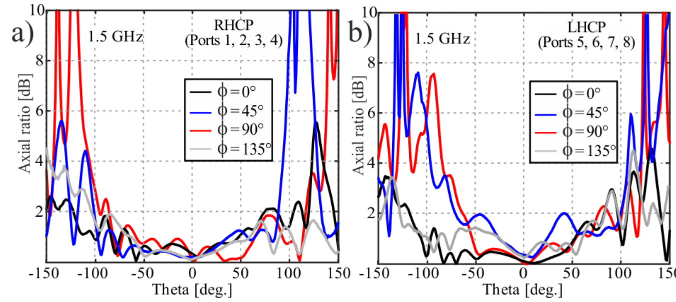

Fig. 16. Design B: measured axial ratios for the RHCP and LHCP states.

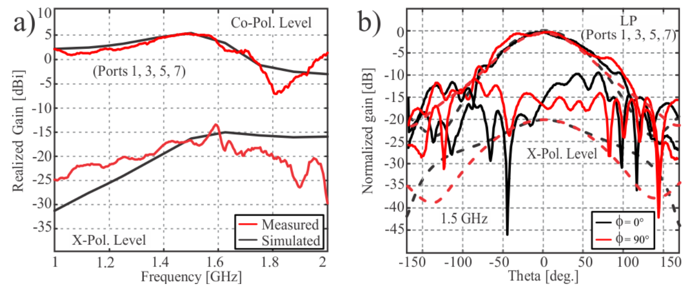

Fig. 17. Design B: LP (vertical) realized gain versus frequency (a) and beam pattern (b). For (b) simulations and measurements are continuous and dashed lines, respectively. Very similar results are observed for Design A, LP (vertical and horizontal) as well as Design B, LP (horizontal). All results not shown for brevity.

Similar challenges were also observed in [29], [30], and [31] where increased cross-polarization levels were observed. These papers mention the importance of the polarization purity for the reference antenna during practical cross-polarization measurements. In addition, there could have been unwanted scattering from the metallic antenna tower and possible twisting of the cabling (acting as an unwanted scattering source) during antenna measurements. Due to these minor setup challenges and the noted polarization impurity in the reference antenna (at L-band [28]) the higher than expected cross-polarization measurement values can be explained. Regardless of these practicalities, measurements and simulations are generally in good agreement for the proposed diversity DRAs.

IV. Conclusion

A novel 8-port dielectric resonator antenna (DRA) was presented for gain and polarization diversity applications. The antenna design consists of eight 50-Ω microstrip lines feeding four slots (with unconventionally two feed lines per slot), and a dielectric resonator element on top with a relative permittivity of $\varepsilon_r = 10$ which exploits degenerate $HE_{11\partial}$ modes. This

0018-926X (c) 2021 Crown Copyright. Personal use is permitted. For any other purposes, permission must be obtained from the IEEE by emailing pubs-permissions@ieee.org.
Authorized licensed use limited to: University of Edinburgh. Downloaded on March 20,2021 at 09:44:49 UTC from IEEE Xplore. Restrictions apply.

This article has been accepted for publication in a future issue of this journal, but has not been fully edited. Content may change prior to final publication. Citation information: DOI 10.1109/TAP.2021.3060034, IEEE Transactions on Antennas and Propagation

DRA structure offers dual-linear and dual-circularly polarized radiation by its flexible port arrangement. Maximum gains of 5.2 dBi and 4.9 dBic are obtained for the linear and circular polarization states, respectively. For proof-of-concept, two distinct prototypes were fabricated and experimentally verified (Design A and Design B). Further advancements could be the realization of a higher dielectric constant for the resonator for size reduction, as briefly studied in [23], as well as an integrated feeding circuit to achieve the different polarization states. Additionally, the feeding system could be modified to provide agile switching between polarization states. The proposed antenna can be used in various communication systems where antenna gain and polarization diversity is required such as in geolocation or other wireless systems.

REFERENCES

[1] Y. Zhou, Y. Jiao, Z. Weng, and T. Ni, "A novel single-fed wide dual-band circularly polarized dielectric resonator antenna," *IEEE Antennas and Wireless Propagation Letters*, vol. 15, pp. 930–933, 2016.

[2] K. Gong and X. H. Hu, "Low-profile substrate integrated dielectric resonator antenna implemented with PCB process," *IEEE Antennas and Wireless Propagation Letters*, vol. 13, pp. 1023–1026, 2014.

[3] Q. Rao, T. A. Denidni, and A. R. Sebak, "Broadband compact stacked T-shaped dra with equilateral-triangle cross sections," *IEEE Microwave and Wireless Components Letters*, vol. 16, no. 1, pp. 7–9, Jan 2006.

[4] T. A. Denidni, Qinjiang Rao, and A. R. Sebak, "Broadband L-shaped dielectric resonator antenna," *IEEE Antennas and Wireless Propagation Letters*, vol. 4, pp. 453–454, 2005.

[5] G. Varshney, V. S. Pandey, R. S. Yaduvanshi, and L. Kumar, "Wide band circularly polarized dielectric resonator antenna with stair-shaped slot excitation," *IEEE Transactions on Antennas and Propagation*, vol. 65, no. 3, pp. 1380–1383, March 2017.

[6] R. Chair, S. L. S. Yang, A. A. Kishk, Kai Fong Lee, and Kwai Man Luk, "Aperture fed wideband circularly polarized rectangular stair shaped dielectric resonator antenna," *IEEE Transactions on Antennas and Propagation*, vol. 54, no. 4, pp. 1350–1352, April 2006.

[7] Chih-Yu Huang, Jian-Yi Wu, and Kin-Lu Wong, "Cross-slot-coupled microstrip antenna and dielectric resonator antenna for circular polarization," *IEEE Transactions on Antennas and Propagation*, vol. 47, no. 4, pp. 605–609, April 1999.

[8] B. Li, C. Hao, and X. Sheng, "A dual-mode quadrature-fed wideband circularly polarized dielectric resonator antenna," *IEEE Antennas and Wireless Propagation Letters*, vol. 8, pp. 1036–1038, 2009.

[9] W. M. Abdel Wahab, D. Busuioc, and S. Safavi-Naeini, "Low cost planar waveguide technology-based dielectric resonator antenna (DRA) for millimeter-wave applications: Analysis, design, and fabrication," *IEEE Transactions on Antennas and Propagation*, vol. 58, no. 8, pp. 2499–2507, Aug 2010.

[10] W. M. Abdel-Wahab, Y. Wang, and S. Safavi-Naeini, "SIW hybrid feeding network-integrated 2-D DRA array: Simulations and experiments," *IEEE Antennas and Wireless Propagation Letters*, vol. 15, pp. 548–551, 2016.

[11] X. Liang and T. A. Denidni, "H-shaped dielectric resonator antenna for wideband applications," *IEEE Antennas and Wireless Propagation Letters*, vol. 7, pp. 163–166, 2008.

[12] M. Abedian, S. K. A. Rahim, and M. Khalily, "Two-segments compact dielectric resonator antenna for UWB application," *IEEE Antennas and Wireless Propagation Letters*, vol. 11, pp. 1533–1536, 2012.

[13] J. H. Winters, J. Salz, and R. D. Gitlin, "The impact of antenna diversity on the capacity of wireless communication systems," *IEEE Transactions on Communications*, vol. 42, no. 234, pp. 1740–1751, Feb. 1994.

[14] B. J. Wysocki, T. A. Wysocki, and J. Seberry, "Modeling dual polarization wireless fading channels using quaternions," in *Joint IST Workshop on Mobile Future, 2006 and the Symposium on Trends in Communications. SympoTIC '06.*, June 2006, pp. 68–71.

[15] R. G. Vaughan and J. B. Andersen, "Antenna diversity in mobile communications," *IEEE Transactions on Vehicular Technology*, vol. 36, no. 4, pp. 149–172, Nov 1987.

[16] J. Moon and Y. Kim, "Antenna diversity strengthens wireless LANs," *Communication Systems Design*, vol. 9, no. 1, pp. 14–24, 2003.

[17] T. Kumberg, R. Tannhaeuser, and L. Reindl, "Wake-up receiver with equal-gain antenna diversity," *Sensors*, vol. 17, p. 1961, 08 2017.

[18] S. K. Yoo, S. L. Cotton, and W. G. Scanlon, "Switched diversity techniques for indoor off-body communication channels: An experimental analysis and modeling," *IEEE Transactions on Antennas and Propagation*, vol. 64, no. 7, pp. 3201–3206, 2016.

[19] S. S. Ikki and M. H. Ahmed, "Performance of cooperative diversity using equal gain combining (EGC) over nakagami-m fading channels," *IEEE Transactions on Wireless Communications*, vol. 8, no. 2, pp. 557–562, 2009.

[20] Y. Gao, Z. Feng, and L. Zhang, "Compact CPW-fed dielectric resonator antenna with dual polarization," *IEEE Antennas and Wireless Propagation Letters*, vol. 10, pp. 544–547, 2011.

[21] Z. Chen, I. Shoaib, Y. Yao, J. Yu, X. Chen, and C. G. Parini, "Pattern-reconfigurable dual-polarized dielectric resonator antenna," *IEEE Antennas and Wireless Propagation Letters*, vol. 15, pp. 1273–1276, 2016.

[22] S. K. Podilchak, M. Clénet, and Y. M. M. Antar, "A hybrid dielectric resonator antenna with polarization-agility and wideband operation," in *The 8th European Conference on Antennas and Propagation (EuCAP 2014)*, April 2014, pp. 3162–3163.

[23] J. C. Johnstone, S. K. Podilchak, M. Clénet, and Y. M. M. Antar, "A compact cylindrical dielectric resonator antenna for MIMO applications," in *2014 IEEE Antennas and Propagation Society International Symposium (APSURSI)*. IEEE, 2014, pp. 1938–1939.

[24] M. V. Kuznetcov, S. K. Podilchak, M. Clénet, and Y. M. M. Antar, "Dielectric resonator antenna with 8-ports for polarization diversity applications," in *IEEE Antennas and Propagation Symposium (APS 2020)*, July 2020 (accepted).

[25] K. U-yen and E. J. Wollack and J. Papapolymerou and J. Laskar, "A Broadband Planar Magic-T Using Microstrip–Slotline Transitions," *IEEE Transactions on Microwave Theory and Techniques*, vol. 56, no. 1, pp. 172–177, 2008.

[26] G. Brzezina and L. Roy, "Miniaturized 180° Hybrid Coupler in LTCC for L-Band Applications," *IEEE Microwave and Wireless Components Letters*, vol. 24, no. 5, pp. 336–338, 2014.

[27] S. K. Podilchak, J. C. Johnstone, M. Caillet, M. Clénet, and Y. M. M. Antar, "A compact wideband dielectric resonator antenna with a meandered slot ring and cavity backing," *IEEE Antennas and Wireless Propagation Letters*, vol. 15, pp. 909–913, 2016.

[28] "Spiral Antennas: Wideband Spiral Antennas: Steatite," 2020. [Online]. Available: https://www.steatite-antennas.co.uk/spiral-antennas/

[29] K. M. Keen and A. K. Brown, "Techniques for the measurement of the cross-polarisation radiation patterns of linearly polarised, polarisation-diversity satellite ground-station antennas," *IEE Proceedings*, vol. 129, no. 3, pp. 103–108, 1982.

[30] Giacomini, A. and Foged, L.J. and Riccardi, A. and Pamp, J. and Cornelius, R. and Heberling, D., "Improving the Cross-Polar Discrimination of Compact Antenna Test Range using the CXR Feed," in *38th Annual Meeting and Symposium of the Antenna Measurement Techniques Association, AMTA*, 2016.

[31] B. T. Walkenhorst and D. Tammen, "Correcting polarization distortion in a compact range feed," in *AMTA 2016 Proceedings*, 2016, pp. 1–6.

0018-926X (c) 2021 Crown Copyright. Personal use is permitted. For any other purposes, permission must be obtained from the IEEE by emailing pubs-permissions@ieee.org.
Authorized licensed use limited to: University of Edinburgh. Downloaded on March 20,2021 at 09:44:49 UTC from IEEE Xplore. Restrictions apply.

This article has been accepted for publication in a future issue of this journal, but has not been fully edited. Content may change prior to final publication. Citation information: DOI 10.1109/TAP.2021.3060034, IEEE Transactions on Antennas and Propagation

Maksim Kuznetcov was born in Kopeysk, Russia, in 1993. He received the M.Eng. degree in electrical and electronic engineering from Heriot-Watt University, Edinburgh, U.K., in 2019. He is currently pursuing the Ph.D. degree with Heriot-Watt University (HWU), Edinburgh, and the University of Edinburgh (UoE), Edinburgh.

In 2019, he joined HWU and UoE as an Research Student, where his research interests include the analysis and design of leaky-wave antennas, duplex antenna systems, and other microwave and antenna technologies.

Symon K. Podilchak (S'03-M'05) received the B.A.Sc. degree in engineering science from the University of Toronto, Toronto, ON, Canada, in 2005, the M.A.Sc. and Ph.D. degrees in electrical engineering from Queen's University, Kingston, in 2008 and 2013, respectively, where he received the Outstanding Dissertation Award for his Ph.D.

From 2013 to 2015, he was an Assistant Professor with Queen's University. In 2015, he joined Heriot-Watt University, Edinburgh, U.K., as an Assistant Professor, and became an Associate Professor in 2017. His research is supported by a H2020 Marie Sklodowska-Curie European Research Fellowship. He is currently a Senior Lecturer with the School of Engineering, The University of Edinburgh, Edinburgh. He is also a registered Professional Engineer (P.Eng.) and has had industrial experience as a computer programmer, and has designed 24 and 77 GHz automotive radar systems with Samsung and Magna Electronics. Recent industry experience also includes the design of high frequency surface-wave radar systems, professional software design and implementation for measurements in anechoic chambers for the Canadian Department of National Defence and the SLOWPOKE Nuclear Reactor Facility. He has also designed new compact multiple-input multiple-output (MIMO) antennas for wideband military communications, highly compact circularly polarized antennas for microsatellites with COM DEV International, and new wireless power transmission systems for Samsung. His research interests include surface waves, leaky-wave antennas, metasurfaces, UWB antennas, phased arrays, and CMOS integrated circuits.

Dr. Podilchak and his students have been the recipient of many best paper awards and scholarships; most notably Research Fellowships from the IEEE Antennas and Propagation Society, the IEEE Microwave Theory and Techniques Society, and the European Microwave Association. He also received a Postgraduate Fellowship from the Natural Sciences and Engineering Research Council of Canada (NSERC) and five Young Scientist Awards from the International Union of Radio Science (URSI). In 2011 and 2013, he received student paper awards at the IEEE International Symposium on Antennas and Propagation, and in 2012, the Best Paper Prize for Antenna Design at the European Conference on Antennas and Propagation for his work on CubeSat antennas, and in 2016, he received the European Microwave Prize for his research on surface waves and leaky-wave antennas. In 2017 and 2019, he was bestowed a Visiting Professorship Award at Sapienza University, Rome, Italy. He was recognized as an Outstanding Reviewer for the IEEE TRANSACTIONS ON ANTENNAS AND PROPAGATION from the IEEE Antennas and Propagation Society in 2014 and 2020. He was also the Founder and First Chairman of the IEEE Antennas and Propagation Society and the IEEE Microwave Theory and Techniques Society, Joint Chapter of the IEEE Kingston Section in Canada and Scotland. In recognition of these services, he was presented with an Outstanding Volunteer Award in May 2015 from IEEE. He currently serves as a Guest Associate Editor for IEEE Open Journal of Antennas and Propagation and IEEE Antennas and Wireless Propagation Letters.

Michel Clénet was born in Nantes, France, in 1968. He received the Master in Sciences and Technology (MST) degree in signal processing and the Diplôme d'Études Approfondies (DEA) degree in telecommunications from the University of Rennes I, France, in 1991 and 1992 respectively, and the PhD. degree in Electrical Engineering from the University of Nantes, France, in 1997.

In 1993, he joined the Electronic and Computer Systems (SEI) Laboratory at IRESTE, Nantes, France, where he was involved in research on antenna systems for mobile communications. He developed several prototypes for adaptive antenna applications. From 1997 to 1999, he was a post-doctoral fellow at the University of Manitoba, Winnipeg, Canada, where he worked on microstrip antennas, arrays and horns. Since 1999, he has been with Defence Research and Development Canada (DRDC), Ottawa, Canada, where he has been working on array signal processing, RF systems, planar antennas, arrays, phased arrays and related technologies, for satellite communication applications. Since 2006, he is leading DRDC activity on controlled reception pattern antenna systems for GPS applications and related technologies.

Michel Clénet is an IEEE senior member. He is currently Adjunct Associate Professor at the Royal Military College of Canada and he is Associate Editor for IET Electronics Letters. He was the Canadian representative for URSI Commission B from 2012 to 2015. Dr. Clénet is author or co-author of 15 journal publications, and of more than 50 communications in international conferences and symposia.

0018-926X (c) 2021 Crown Copyright. Personal use is permitted. For any other purposes, permission must be obtained from the IEEE by emailing pubs-permissions@ieee.org.
Authorized licensed use limited to: University of Edinburgh. Downloaded on March 20,2021 at 09:44:49 UTC from IEEE Xplore. Restrictions apply.

This article has been accepted for publication in a future issue of this journal, but has not been fully edited. Content may change prior to final publication. Citation information: DOI 10.1109/TAP.2021.3060034, IEEE Transactions on Antennas and Propagation

Yahia M.M. Antar Yahia M. M. Antar (Life Fellow, IEEE) received the B.Sc. degree (Hons.) from Alexandria University, Alexandria, Egypt, in 1966, and the M.Sc. and Ph.D. degrees from the University of Manitoba, Winnipeg, MB, Canada, in 1971 and 1975, respectively, all in electrical engineering.,In May 1979, he joined the Division of Electrical Engineering, National Research Council of Canada, Ottawa, ON, Canada.

In November 1987, he joined the Department of Electrical and Computer Engineering, Royal Military College of Canada, Kingston, ON, where he has been a Professor since 1990. He has authored or coauthored over 200 journal articles, several books, and chapters in books, over 450 refereed conference papers, holds several patents, has chaired several national and international conferences, and has given plenary talks at many conferences.

Professor Antar was appointed as a member of the Canadian Defense Advisory Board (DAB) of the Canadian Department of National Defense in January 31, 2011. He is a fellow of the Engineering Institute of Canada (FEIC) and the Electromagnetic Academy. He is also an International Union of Radio Science (URSI) Fellow. In 1977, he holds a Government of Canada Visiting Fellowship at the Communications Research Centre, Ottawa. In 2003, he was awarded the Royal Military College of Canada “Excellence in Research” Prize and the RMCC Class of 1965 Teaching Excellence award in 2012. He was elected by the URSI to the Board as the Vice President in August 2008 and 2014 and to the IEEE Antennas and Propagation (AP-S) AdCom. In 2019 Professor Antar was elected as the 2020 president-elect for IEEE AP-S, and will serve as president in 2021.

In October 2012, he received the Queen’s Diamond Jubilee Medal from the Governor General of Canada in recognition for his contribution to Canada. He was a recipient of the 2014 IEEE Canada RA Fessenden Silver Medal for Ground Breaking Contributions to Electromagnetics and Communications and the 2015 IEEE Canada J. M. Ham Outstanding Engineering Education Award. In May 2015, he received the Royal Military College of Canada Cowan Prize for excellence in research. He was also a recipient of the IEEE-AP-S of the Chen-To-Tai Distinguished Educator Award in 2017.

He served as the Chair for Canadian National Commission (CNC), URSI, from 1999 to 2008, Commission B from 1993 to 1999, and has a cross appointment at Queen’s University, Kingston. In May 2002, he was awarded the Tier 1 Canada Research Chair in electromagnetic engineering which has been renewed in 2016. He has supervised and co-supervised over 90 Ph.D. and M.Sc. theses at the Royal Military College and at Queen’s University, several of which have received the Governor General of Canada Gold Medal Award, the Outstanding Ph.D. Thesis of the Division of Applied Science, as well as many Best Paper Awards in major international symposia. He also has served as an Associate Editor for many IEEE and IET Journals and an IEEE-APS Distinguished Lecturer.

0018-926X (c) 2021 Crown Copyright. Personal use is permitted. For any other purposes, permission must be obtained from the IEEE by emailing pubs-permissions@ieee.org.
Authorized licensed use limited to: University of Edinburgh. Downloaded on March 20,2021 at 09:44:49 UTC from IEEE Xplore. Restrictions apply.